Linking brain-heart interactions to emotional arousal in immersive virtual reality

Fourcade A. (1, 2, 3, 4)*, Klotzsche, F. (2, 3), Hofmann, S. M. (2, 5), Mariola, A. (6, 7), Nikulin, V. V. (2), Villringer A. (1, 2, 3, 4) and Gaebler M. (2, 3)

(1) Max Planck School of Cognition, Stephanstrasse 1a, Leipzig, Germany

(2) Department of Neurology, Max Planck Institute for Human Cognitive and Brain Sciences, Leipzig, Germany

(3) Humboldt-Universität zu Berlin, Faculty of Philosophy, Berlin School of Mind and Brain

(4) Charité - Universitätsmedizin Berlin, Germany

(5) Department of Artificial Intelligence, Fraunhofer Institute Heinrich-Hertz, Berlin, Germany

(6) Sussex Neuroscience, School of Life Sciences, University of Sussex, Brighton, United Kingdom

(7) School of Psychology, University of Sussex, Brighton, United Kingdom

*e-mail: antonin.fourcade@maxplanckschools.de

Data availability

We did not obtain participants' consent to release their individual data. Since our analyses focus on the single-subject level, we have only limited data which are sufficiently anonymized (e.g., summarized or averaged) to be publicly shared. Wherever possible, we provide "source data" to reproduce the manuscript's tables and figures. All code used for all analyses and plots are publicly available on GitHub at https://github.com/afourcade/evrbhi.

Acknowledgements

This research was supported by the Max Planck Dahlem Campus of Cognition (MPDCC) and funded by the Max Planck Society - Fraunhofer-Gesellschaft cooperation (project “NEUROHUM”) and the German Federal Ministry of Education and Research (BMBF grant 13GW0488).

Author contributions

F.K., S.M.H., A.M. and M.G. conceived the original experiment, performed data acquisition and provided data. M.G. and A.F. developed the analyses. V.N. and A.V. advised analyses. A.F. wrote the analysis code, analyzed the data and wrote the first draft of the manuscript. All authors edited the manuscript.

Competing interests

The authors declare no competing interests.

Abstract

The subjective experience of emotions is rooted in the contextualized perception of changes in bodily (e.g., heart) activity. Increased emotional arousal (EA) has been related to lower high-frequency heart rate variability (HF-HRV), lower EEG parieto-occipital alpha power, and higher heartbeat-evoked potential (HEP) amplitudes. We studied EA-related brain-heart interactions (BHIs) using immersive virtual reality (VR) for naturalistic yet controlled emotion induction. 29 healthy adults (13 women, age: 26±3) completed a VR experience that included rollercoasters while EEG and ECG were recorded. Continuous EA ratings were collected during a video replay immediately after. We analyzed EA-related changes in HF-HRV as well as in BHIs using HEPs and directional functional BHI modeling.

Higher EA was associated with lower HEP amplitudes in a left fronto-central electrode cluster. While parasympathetic modulation of the heart (HF-HRV) and parieto-occipital EEG alpha power were reduced during higher EA, there was no evidence for the hypothesized EA-related changes in bidirectional information flow between them. Whole-brain exploratory analyses in additional EEG (delta, theta, alpha, beta and gamma) and HRV (low-frequency, LF, and HF) frequency bands indicated a temporo-occipital cluster, in which higher EA was linked to decreased brain-to-heart (gamma→HF-HRV) and increased heart-to-brain (LF-HRV→gamma) information flow. Our results confirm previous findings from less naturalistic experiments and suggest EA-related BHI changes in temporo-occipital gamma power.

Introduction

Emotions result from internal or external events that are appraised as relevant to an organism's well-being (Gross, 1998; Rottenberg & Gross, 2003). Emotions have subjective and physiological components (Mauss & Robinson, 2009), among others (e.g., expressive; Sander et al., 2005). We aimed to link subjective emotional experience to physiological activity not only in the brain but also in the heart and their interaction under naturalistic stimulation using immersive virtual reality.

The subjective component of emotions or - more generally - of affect is a basic property of human experience (Wundt, 1897) or consciousness (Barrett, 2016), and it is rooted in the contextualized perception of bodily changes (James, 1884; Lange, 1885). That is, interoceptive information (e.g., autonomic, visceral) about the physiological state of the internal body (Craig, 2002; Barrett, 2016) is combined with exteroceptive information (e.g., auditory, visual) about the physical state of the external world. The subjective experience of affect is often described using the two continuous dimensions or "core affects" of valence and *emotional* arousal (EA; Russell, 2003): Valence refers to how pleasant or unpleasant, and EA refers to how intense the experience is (Barrett & Russell, 1999).

Sweaty palms, increased heart rate, and the throat tightening at the sight of a snake are examples of physiological responses connected to emotions. These peripheral physiological responses are regulated by the autonomic nervous system (ANS), with activity of the parasympathetic branch of the ANS being linked to rest and digestion and activity of the sympathetic branch to the "flight-or-fight" response (McCorry, 2007). Focusing on the cardiovascular response, the two branches can modulate the activity of the sinoatrial node in the heart and change the heart rate (Levy, 1971). These influences have different temporal dynamics, with sympathetic regulation being relatively

slow (at the order of seconds) and parasympathetic regulation being relatively fast (at the order of milliseconds; Warner & Cox, 1962; Levy & Martin, 1984). While isolating the sympathetic influence on the heart has been difficult (Goldstein et al., 2011; Reyes del Paso et al., 2013; Shaffer et al., 2014), the parasympathetic influence, or vagal cardioregulation, can be quantified by high-frequency heart rate variability (HF-HRV; Task Force, 1996). HRV refers to the fluctuations of the time between heartbeats (i.e., the interbeat interval, IBI), and its HF component (typically between 0.15 and 0.4 Hz) captures the rapid IBI changes caused by changes in parasympathetic activity - whereas its low frequency component (LF-HRV; typically between 0.04 and 0.15 Hz) reflects both sympathetic and parasympathetic influence on the heart. Autonomic and heart activity have been linked to emotion, but specific patterns that are exclusively associated with particular emotion categories could not be identified (Kreibig, 2010; Siegel et al., 2018). For the dimensional core affects of EA and valence, changes in autonomic or heart activity appear more consistently in the literature; unpleasant (i.e., negatively valenced) stimuli (e.g., movie, music) were associated with a decrease in heart rate (Palomba et al., 2000; Sammler et al., 2007) and higher EA was linked to decreased HF-HRV (Valenza et al., 2012; Luft & Bhattacharya, 2015; Hildebrandt et al., 2016), suggesting a decreased parasympathetic influence on the heart during higher EA.

The integration of external (exteroceptive) and internal (interoceptive) signals (e.g., from the heart), which gives rise to emotional experiences, takes place in the brain (Craig, 2009; Seth, 2013). The two autonomic branches transmit sensory signals from the heart (e.g., via the vagus nerve, through the dorsal root and stellate ganglia; Dusi & Ardell, 2020) to the brainstem, where they are relayed to the cerebrum and cerebellum. Reversely. preganglionic autonomic motor neurons are also controlled by the brain; in particular by the central autonomic network (CAN), which includes the hypothalamus, amygdala, anterior cingulate, insula and medial prefrontal

cortex (Benarroch, 1993; Thayer & Lane, 2000, 2009). These brain regions are also consistently reported in neuroimaging studies of emotions (Dalgleish, 2004; Lindquist et al., 2012). Recent causal evidence from rodents suggests that insula and brainstem circuits in particular integrate cardiac activity into information processing, influencing perception and behavior (Gehrlach et al., 2019; Hsueh et al., 2023; Klein et al., 2021; Signoret-Genest et al., 2023).

The activation in the heart and the brain can be electrophysiologically recorded using ECG and EEG, respectively. Both signals contain oscillatory and aperiodic components (heart: Babloyantz & Destexhe, 1988; brain: Buzsáki et al., 2013; He, 2014). In the ECG signal, oscillations in HRV are typically decomposed into LF- and HF-HRV, while in the EEG signal, five frequency bands are commonly defined: delta (δ; 0.3–4 Hz), theta (θ; 4–8 Hz), alpha (α; 8–13 Hz), beta (β; 13–30 Hz) and gamma (γ; 30–45 Hz). Various functions, from more fundamental sensory and motor to higher cognitive processes, have been ascribed to different types of regionally distributed neural oscillations (Buzsaki, 2006). In particular, the parieto-occipital alpha rhythm is the dominant EEG rhythm in awake adults with eyes closed (Berger, 1929), where it varies with vigilance (Olbrich et al., 2009). Its physiological bases are large-scale synchronization of neuronal activity (Buzsaki, 2006) and metabolic deactivation (Moosmann et al., 2003). Psychophysiologically, parieto-occipital alpha power is correlated to EA (Koelstra et al., 2012; Luft & Bhattacharya, 2015; Hofmann, Klotzsche, Mariola et al., 2021), as well as to attentional processes (Klimesch, 2012; van Diepen et al., 2019) which help prioritize and select sensory inputs (Treisman, 1969; Driver, 2001). Particularly bottom-up or stimulus-driven attention is assumed to direct perception towards a subset of salient external stimuli (Egeth & Yantis, 1997).

Besides sharing an electrophysiological pattern, affect and attention have been psychologically linked. On the one hand, emotional stimuli capture attentional focus (Nummenmaa et al., 2006,

2009) and their processing is prioritized over non-emotional stimuli (Okon-Singer et al., 2013). On the other hand, changes in affective states (and particularly the level of EA) alter attention-related changes in salience also for non-emotional stimuli (Sutherland & Mather, 2018). As a side node, the CAN overlaps with the salience network (SN; Menon, 2015; Seeley, 2019), which is involved in directing attention towards (e.g., emotionally) relevant stimuli (Vuilleumier, 2005; Menon & Uddin, 2010).

In sum, as activity in the heart and the brain separately play important roles for affective experiences, their multimodal or joint analysis promises to capture the physiology of human experience more comprehensively than the analysis of either of the modalities alone (e.g., Raimondo et al., 2017). Emotion-related brain-heart interactions (BHIs), typically measured through electrophysiological recordings, have been investigated using different methodologies: for instance, by means of event-related (e.g., heartbeat-evoked potentials [HEP]; Luft & Bhattacharya, 2015) and oscillatory analyses (e.g., directional functional BHI: Candia-Rivera et al., 2022).

The HEP is an event-related potential (ERP) component that can be observed when the EEG signal is time-locked to the R-peaks in the ECG (Schandry et al., 1986). The HEP is taken to reflect the cortical processing of the heartbeat (Park & Blanke, 2019) and its amplitude is modulated by interoceptive (Pollatos et al., 2016) and emotional processing. For example, Luft and Bhattacharya (2015) manipulated EA through videos and music (NB: without assessing subjective experience) and found higher HEP amplitudes during blocks of higher (HA) compared to lower EA (LA) - particularly over right parietal electrodes (P6 and P8) from 0.38 to 0.46 s after the R-peak. Higher HEP amplitude has been interpreted as reflecting a shift of attentional focus from external stimuli to internal bodily states (García-Cordero et al., 2017; Villena-González et al., 2017; Petzschner et al., 2019; Zaccaro et al., 2022).

Directional functional BHI can be computed by jointly analyzing oscillations in EEG and ECG data, for example with the synthetic data generation (SDG) model (Catrambone et al., 2019). Based on the assumption of a bidirectional communication loop in which ongoing HRV (as a proxy for ANS activity) modulates EEG activity and, in turn, ongoing EEG activity modulates HRV, the SDG combines generative models for the EEG and the heartbeat. Using this approach, Candia-Rivera and colleagues (2022) recently found that the ascending information flow from the vagal cardioregulation (i.e., HF-HRV) to the EEG oscillations in the delta, theta, and gamma bands correlated with EA ratings, particularly in frontal and parieto-occipital electrodes. Furthermore, higher ascending heart-to-brain information flow preceded lower descending brain-to-heart information flow and these EA-related changes in BHI were associated with HF-HRV but not LF-HRV (Candia-Rivera et al., 2022).

Besides advances in the multimodal analysis of physiological signals, affective neuroscience is currently experiencing advances in emotion elicitation. Past research has extensively used static images repeatedly presented in trial-based designs, often creating an artificial and discontinuous experience (Bridwell et al., 2018; Huk et al., 2018). However, affective phenomena, along with their associated physiological responses, are varying on different continuous time scales; for example, EA can fluctuate on the order of minutes (Kuppens et al., 2010) or seconds (Mikutta et al., 2012). Dynamic stimuli that capture such naturalistic fluctuations in affective experience could be videos (Samide et al., 2020) or even emotional stimuli in everyday life (Grosse Rueschkamp et al., 2019). While the former remain relatively artificial (e.g., non-interactive), the latter are difficult to experimentally control (e.g., comprehensively measure). Immersive Virtual Reality (VR; wherein the user is surrounded by the virtual environment) presents a trade-off between naturalism and experimental control (Bohil et al., 2011) and offers several advantages: It enables (1) the

creation and presentation of computer-generated scenarios that are contextually rich and engaging (Diemer et al., 2015), (2) naturalistic elicitation of specific psychological states (which may be particularly relevant for affective states; Baumgartner et al., 2006; Riva et al., 2007; Dores et al., 2014; Meuleman & Rudrauf, 2021), and (3) the recording of multimodal measurements (e.g., subjective ratings, movements, heart and brain signals) - with more experimental control (and less noise) than in real-life assessments (Meuleman & Rudrauf, 2021).

Recently, we used an emotionally arousing VR experience (including two rollercoasters with a break in-between) while EEG and ECG were recorded and EA was continuously rated (Hofmann, Klotzsche, Mariola et al., 2021). Using spatial filtering and non-linear machine learning for the analysis of the EEG data, we could decode subjective EA from parieto-occipital alpha power. Given the importance of cardiac activity and the heart-brain axis for affective experience and EA, we now included the ECG into the analysis. We thereby expected the joint analysis to offer insights about the physiology of EA that are not accessible when investigating EEG signals alone. In particular, we investigated the role of vagal cardioregulation for the EEG alpha power reduction during HA compared to LA, and our hypotheses were:

1. Cardiac activity and vagal cardioregulation (indexed by IBIs and HF-HRV, respectively) differ between states of HA and LA.
2. HEP amplitudes differ between states of HA and LA, particularly around 400 ms after a heartbeat and in right temporo-parietal electrodes (based on Luft & Bhattacharya, 2015).
3. EA-related changes in parieto-occipital alpha oscillations (Hofmann, Klotzsche, Mariola et al., 2021) are related to changes in heart activity (i.e., HF-HRV).

Methods

1. Participants

Participants were recruited via the participant database at the Berlin School of Mind and Brain (an adaptation of ORSEE; Greiner, 2015). Inclusion criteria were right-handedness, normal or corrected-to-normal vision, proficiency in German, no (self-reported) psychiatric, or neurological diagnoses in the past 10 years, and less than 3 hr of experience with VR. Participants were requested not to drink coffee or other stimulants 1 hr before coming to the lab. The experiment took ~2.5 hr, and participants were reimbursed with 9 € per hour. They signed informed consent before their participation, and the study was approved by the Ethics Committee of the Department of Psychology at the Humboldt-Universität zu Berlin. Forty-five healthy young adults (22 men, mean age: 23±4, range: 20-32 years) came to the lab. Data from eleven participants needed to be discarded due to technical problems (n = 5), electrode malfunctioning (EEG: n = 1, ECG: n = 3), discontinuation of the experiment (n = 1) or violation of inclusion criteria (n = 1), so that data from 34 participants were processed. After EEG quality assurance (details below), data from 29 participants (16 men, mean age: 26±3, range: 20-31 years) entered the analyses.

2. Materials

EEG (sampled at 500 Hz, hardware-based low-pass filter at 131 Hz) was recorded with 30 active Ag/AgCl electrodes attached according to the international 10-20 system (actiCap and LiveAmp, Brain Products GmbH, Germany) and referenced to electrode FCz. Two additional electrodes captured eye movements (electrooculography) and were placed below and next to the right eye.

ECG was synchronously recorded (sampled at 500 Hz) with additional electrodes in a bipolar Lead I configuration. A grounding electrode was placed on the right clavicle and two passive lead electrodes were positioned bilaterally on the participant's torso (lower rib cage). In addition, skin conductance was recorded at the index and annulary fingers of the left hand (data not considered here).

VR setup: A HTC Vive HMD (HTC, Taiwan) with headphones was attached on top of the EEG cap using cushions to avoid pressure artifacts. The VR experience was commercially available on Steam ("Russian VR Coasters" by Funny Twins Games, 2016).

3. Design and Procedure

Participants had a 280-s VR experience, which included two rollercoasters (153 s, 97 s) and a 30-s intermediate break, twice: once keeping their head straight to avoid movement-related artifacts in the EEG data (*nomov* condition) and once freely moving their head (*mov* condition). The order was randomized across participants (in the 29 analyzed, *nomov-mov*: $n = 13$; *mov-nomov*: $n = 16$). In the subsequent rating phase (following immediately after the VR experience for each movement condition), the participants saw a 2D recording of their experience on a virtual screen. While viewing the video, the participants recalled their EA and continuously reported it using a dial (Griffin PowerMate USB; sampling frequency: 50 Hz), with which they manipulated a vertical rating bar next to the video, ranging from low (0) to high (50) EA (McCall et al., 2015). For further details of the experimental setup and data acquisition procedures, please refer to Hofmann, Klotzsche, Mariola et al. (2021).

4. Preprocessing

An overview of the preprocessing steps is presented in Figure 1. The preprocessing steps were applied separately for data recorded during the *nomov* and *mov* conditions (i.e., without and with head movement, respectively).

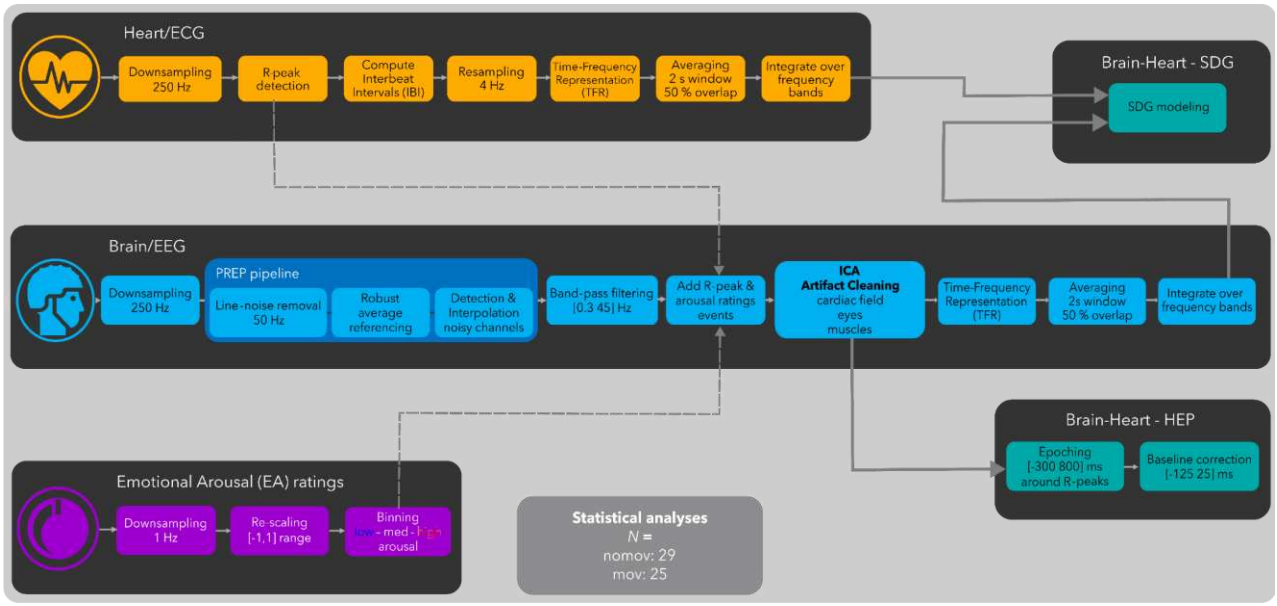

Figure 1. *Flowchart of the preprocessing pipeline. Emotional arousal (EA) ratings (in purple), Heart/ECG (in orange), Brain/EEG (in blue), Brain-Heart (in turquoise): Heart-evoked potentials (HEP) and synthetic data generation (SDG) modeling; Please note that TFR computation and SDG modeling was preceded by symmetric padding. Further details of the preprocessing steps can be found in the corresponding sections.*

4.1. Data Cropping

EEG data, ECG data, and retrospective arousal ratings were cropped by 10 s (2.5 s at beginning and 2.5 s at end of each rollercoaster) to avoid outliers related to the onset and offset of the virtual rollercoaster rides. This resulted in two time series (*nomov, mov*) of 270 s per participant.

4.2. Emotional Arousal (EA) Ratings

Subjective reports were downsampled to 1 Hz by averaging non-overlapping sliding windows and rescaled to a [-1 1] range. The ratings were then divided by a tertile split into three distinct bins of arousal ratings (low, medium, high) per participant. The medium arousal ratings were discarded, resulting in 180 samples per subject (90 for low, 90 for high EA).

4.3. Heart/ECG

ECG recordings were downsampled to 250 Hz. Automatic R-peak detection and manual inspection/correction was performed with the EEGLAB extension HEPLAB (version 1.0.1; Perakakis, 2019) in MATLAB (version R2022a).

IBI time series were computed, resampled to 4 Hz (cubic-spline interpolation) and their time-frequency representation (TFR) performed using Continuous Wavelet Transform (CWT, mother wavelet: Morlet, $\omega_0 = 6$), using the neurokit2 package (version 0.2.3; Makowski et al., 2021) in Python (version 3.10). To this end, to minimize artifacts due to semi-continuity (i.e., transition effects at the beginning and end of the break), the first R-peak after the beginning and end of the break were removed before resampling. To minimize edge artifacts at the beginning and end of the time-series, a symmetric padding (70 s of inverted data, concatenated at the beginning and end of time-series) was added to the IBI time-series before computing CWT.

The TFRs were downsampled to 1 Hz by averaging within a sliding window of 2 s and 50 % overlap. High and low heart rate variability spectral-power time series were derived by integrating TFRs within the frequency ranges 0.04–0.15 Hz (LF-HRV) and 0.15–0.4 Hz (HF-HRV). Finally, the symmetric padding was partially removed from the IBI and HRV time-series, keeping 35 s of symmetric padding in order to initialize the SDG models (see below).

4.4. Brain/EEG

EEG data were preprocessed and analyzed with custom MATLAB and Python scripts building on the EEGLAB toolbox (version 2023.0; Delorme & Makeig, 2004) and MNE (version 1.1.0; Gramfort et al., 2013; Larson et al., 2022). Continuous data were downsampled to 250 Hz and PREP pipeline (v.0.56.0; Bigdely-Shamlo et al., 2015) procedures were applied for line-noise removal (line frequency: 50 Hz), robust referencing to average, and detection as well as spherical interpolation of noisy channels. On average, 2.08 and 2.47 channels per subject were interpolated in the *nomov* and *mov* condition, respectively. Data were then bandpass filtered (0.3–45 Hz; Hamming windowed sinc FIR filter). Retrospective arousal ratings and R-peak timings were added as event markers to the data sets.

ICA (Extended infomax; Lee et al., 1999) decomposition was used to identify and remove EEG artifacts caused by eye movements, blinks, cardiac field artifacts (CFA) and muscular activity. To facilitate the decomposition, ICA projection matrices were calculated on a copy of the data, high-pass filtered at 1 Hz (instead of 0.3 Hz; Winkler et al., 2015) and from which the noisiest parts had been removed. To this end, a copy of the continuous data was split into 270 epochs of 1 s length. Epochs containing absolute voltage values > 100 µV in at least one channel (excluding channels that reflected eye movements, i.e., EOG channels, Fp1, Fp2, F7, F8) were deleted. Extended infomax (Lee et al., 1999) ICA decomposition was calculated on the remaining parts of the data (after correcting for rank deficiency with a principal component analysis). Subjects with > 90 to-be-deleted epochs (33 % of the data) were discarded from further analyses (*nomov*: $n = 5$; *mov*: $n = 9$). Artefactual ICA components were semi-automatically selected using the SASICA extension (version 1.3.8; Chaumon et al., 2015) of EEGLAB and visual inspection. On average, 10.51 (*nomov;* eye: 2.97, muscle: 4.79, CFA: 1.21, other: 1.45) and 13.40 (*mov;* eye: 3.36, muscle: 5.84,

CFA: 1.01, other: 2.92) components per subject were discarded. The remaining ICA weights were back-projected onto the continuous time-series.

TFRs were calculated using Continuous Wavelet Transform (CWT; mother wavelet: Morlet, number of cycles = 7). To minimize edge artifacts and transition effects, CWT was computed on each section separately (roller coaster 1, break, roller coaster 2) with a symmetric padding and then re-concatenated together.

The resulting TFRs were downsampled to 1 Hz by averaging within a moving window of 2 s and 50 % overlap. The EEG spectral power time-series at each electrode were derived by integrating the TFRs within the five classical frequency bands: delta (δ; 0.3–4 Hz), theta (θ; 4–8 Hz), alpha (α; 8–13 Hz), beta (β; 13–30 Hz) and gamma (γ; 30–45 Hz). Thirty-five seconds of symmetric padding at the beginning of the time-series was kept to initialize the SDG models (see below).

4.5. Brain-Heart

In addition to the preprocessing steps described above, additional processing steps were applied for the joint analysis of heart and brain signals:

4.5.1. Heartbeat-Evoked Potentials (HEP)

In the time domain, the preprocessed EEG data were epoched, from 300 ms before each R-peak to 800 ms after. Epochs were then baseline corrected by subtracting for each epoch the mean voltage in the time-window [-125 -25] ms.

4.5.2. Synthetic Data Generation (SDG)

IBI, LF-HRV, HF-HRV, and alpha spectral power time-series for each subject and head movement condition were used as inputs for the SDG model (Catrambone et al., 2019).

In this approach, the ECG R-peaks are modeled (based on integral pulse frequency modulation; Brennan et al., 2002) as a sequence of Dirac delta functions, which are generated by integrating the activity of two oscillators (one for each HRV frequency band: LF and HF) representing the autonomic regulation of the heart activity. Crucially, the amplitudes of the oscillators depend on an additional brain-to-heart coupling coefficient. This coefficient quantifies the strength of the information flow from a specific EEG frequency band to a specific HRV frequency band. The EEG signal, in turn, is modeled (based on adaptive Markov process amplitude; Al-Nashash et al., 2004) as multiple oscillators (one for each frequency band: delta, theta, alpha, beta, gamma), whose amplitudes depend on an additional heart-to-brain coupling coefficient. This coefficient quantifies the strength of the information flow from a specific HRV frequency range to a specific EEG frequency range. Therefore, both EEG and HRV time-series are mutually dependent, and their interaction is modulated by the introduced coupling coefficients. Finally, by means of inverse modeling, both brain-to-heart and heart-to-brain coupling coefficients can be derived.

As model parameters, a 15 s long time window with a 1 s step was used to estimate the coefficients, and the central frequencies used were $\omega s = 2\pi \cdot 0.1\ rad/s$ (LF band central frequency = 0.1 Hz) and $\omega p = 2\pi \cdot 0.25\ rad/s$ (HF band central frequency = 0.25 Hz). The output of the model was the time courses of the coupling coefficients, in both direction (i.e., brain-to-heart and heart-to-brain), for all combinations of brain oscillations (delta, theta, alpha, beta, and gamma) and HRV components (LF and HF).

Please note that with these parameters, the SDG model needed 30 s to initialize. To avoid missing data for the first 30 s of the VR experience, all the inputs had 35 s of symmetric padding added at the beginning and end. This symmetric padding was kept from the previous preprocessing steps (TFR computation).

5. Statistical Analysis

5.1. Selection of Region of Interest (ROI)

Based on previous findings (Hofmann, Klotzsche, Mariola et al., 2021; Candia-Rivera et al., 2022), we focused on the interaction between alpha power and HF-HRV, in all parieto-occipital electrodes. We therefore defined a ROI including the following EEG electrodes: Pz, P3, P4, P7, P8, O1, O2, and Oz.

5.2. Heart/ECG

From the IBI and HRV time-series, time-points corresponding to low and high arousal ratings were selected and entered into linear mixed models (LMM; lme4 [version 1.1-29] and lmerTest [version 3.1-3] packages in R [version 4.1.0]; Bates et al., 2014; Kuznetsova et al., 2017), with two factors: (emotional) arousal (two levels: high, low); and (head) movement (two levels: nomov, mov). HRV values were log-transformed in order to approximate a normal distribution.

Each factor and their interaction were entered both as fixed and random effect (i.e., full model; Barr et al., 2013), as follows:

$$\text{IBI or } \log(\text{HRV}) \sim 1 + \text{arousal} + \text{movement} + \text{arousal} * \text{movement} + (1 + \text{arousal} + \text{movement} + \text{arousal} * \text{movement} \mid \text{ID})$$

In the fixed effects, an intercept and slopes for the two factors and their interaction were estimated. In the random effects, an intercept and slopes for the two factors and their interaction were estimated within participants.

318 *P*-values for *F*- and *t*-tests were calculated using the lmerTest ANOVA (type 3) function using
319 Satterthwaite's method. Estimated marginal means (with 95% confidence intervals) and post hoc
320 pairwise comparisons (with Tukey correction for *p*-values) were computed using the emmeans
321 package (version 1.7.3; Lenth, n.d.).

322 ### 5.3. Brain/EEG

323 For each participant and each head movement condition, alpha spectral power was averaged over
324 the electrode ROI. From the alpha spectral power time-series, time-points corresponding to low
325 and high arousal ratings were selected and entered into the same LMM as for the Heart/ECG
326 analysis, with two factors: (emotional) arousal (two levels: high, low); and (head) movement (two
327 levels: nomov, mov). Alpha power values were log-transformed in order to approximate a normal
328 distribution.
329 Each factor and their interaction were entered both as fixed and random effect, as follows:

330 $\log(\alpha) \sim 1 + \text{arousal} + \text{movement} + \text{arousal} * \text{movement}$

331 $+ (1 + \text{arousal} + \text{movement} + \text{arousal} * \text{movement} \mid \text{ID})$

332 ### 5.4. Brain-Heart

333 #### 5.4.1. HEP

334 In a whole-head analysis, non-parametric cluster-based permutation t-tests were used to compare
335 HEP amplitudes between HA and LA between 250 ms and 450 ms after R-peaks, by pooling the
336 data from both head movement conditions. Previous studies (e.g., Schandry et al., 1986; Al et al.,
337 2020) typically reported HEPs between 250 and 400 ms; we extended this time-window to 450 ms
338 to include Luft and Battacharya (2015) findings. A cluster threshold of $p = .05$ (for clustering data

339 points temporally and spatially adjacent) and 10,000 random permutations (to create the null
340 distribution) were used. Clusters with $p < .05$ (two-tailed) in the permutation test were considered
341 significant.

342 #### 5.4.2. SDG

343 For each participant and each head movement condition, heart-to-brain and brain-to-heart
344 couplings (model outputs HF-HRV → α and α → HF-HRV, respectively) were averaged over the
345 electrode ROI. Time-points corresponding to low and high arousal ratings were selected and
346 entered into the same LMM as for the Heart/EEG and Brain/EEG analyses, with two factors:
347 (emotional) arousal (two levels: high, low); and (head) movement (two levels: nomov, mov).
348 Coupling values were log-transformed in order to approximate a normal distribution.
349 Each factor and their interaction were entered both as fixed and random effect, as follows:

350 log(HF-HRV → α) or log(α → HF-HRV) ~ 1+ arousal + movement + arousal * movement

351 + (1+ arousal + movement + arousal * movement | ID)

352 ## 6. HEP Source Localization

353 Exact low-resolution tomography analysis (eLORETA, RRID:SCR_007077; Pascual-Marqui,
354 2007) was used to localize the sources corresponding to HEP differences between HA and LA.
355 Our pipeline was based on the work of Idaji et al., 2020, who customized the eLORETA
356 implementation of the M/EEG Toolbox of Hamburg (https://www.nitrc.org/projects/meth/). Our
357 forward model was constructed via the New York Head model (Haufe et al., 2014; Huang et al.,
358 2016; Haufe & Ewald, 2019) with approximately 2000 voxels and by using 28 out of 30 scalp
359 electrodes (TP9 and TP10 were removed because they are not contained in the model). Crucially,

we constrained our sources to be perpendicular to the cortical surface. Individual HA vs. LA scalp activations were taken as the averaged topography of the difference of HEPs between HA and LA within the time-window of observed EA-related HEP differences at the group level (328 to 360 ms after R-peak, based on the cluster-based permutation testing). Inverse modeling was computed separately per participant and the L2-normalized source activations were then averaged across all subjects.

7. Control and Exploratory Analyses

To test the robustness of our methods and the specificity of our results, we conducted several control analyses.

7.1. ECG Waveform

To control for potential confounds in our HEP results, we tested for possible differences in the ECG waveforms between HA and LA. We compared the ECG signal time-locked to the R-peak of HA vs. LA within participants, using two-tailed paired t-tests at all time-points within the time-window of observed EA related HEP differences. The *p*-value was corrected for multiple comparisons with False Discovery Rate (FDR; Benjamini & Yekutieli, 2001).

7.2. Other frequency bands

To evaluate the specificity of the effects in the alpha band and explore arousal-related changes in (A) brain activity and (B) BHI (Candia-Rivera et al., 2022), we performed a whole-scalp analysis for (A) all the EEG frequency bands: delta (δ; 0.3–4 Hz), theta (θ; 4–8 Hz), alpha (α; 8–13 Hz), beta (β; 13–30 Hz) and gamma (γ; 30–45 Hz), and (B) their integration in SDG (LF-HRV → δ, δ → LF-HRV, HF-HRV → δ, δ → HF-HRV; LF-HRV → θ, θ → LF-HRV, HF-HRV → θ, θ →

381 HF-HRV; LF-HRV → α, α → LF-HRV, HF-HRV → α, α → HF-HRV; LF-HRV → β, β → LF-
382 HRV, HF-HRV → β, β → HF-HRV; LF-HRV → γ, γ → LF-HRV, HF-HRV → γ, γ → HF-
383 HRV). To this end, at each electrode, we averaged the different metrics over the head movement
384 conditions, and performed paired t-tests between the mean during HA and the mean during LA
385 for each participant.

Results

1. Participants

After the EEG quality assurance during preprocessing, the data from 29 participants (16 men, mean age: 26±3, range: 20-31 years) entered the subsequent analyses. More specifically, after excluding 5 (*nomov*) and 9 (*mov*) participants, results were based on : $N_{nomov} = 29$ and $N_{mov} = 25$.

2. Heart/ECG

There was a significant main effect of arousal ($F(1, 28.6) = 5.9$, $p = .021$) on HF-HRV (see Figure 2). No evidence for a main effect of head movement ($F(1, 24.6) = 1.6$, $p = .218$), nor the interaction ($F(28.1) = 1.4$, $p = .245$) was found. Post-hoc pairwise comparisons of the estimated marginal means revealed significantly lower HF-HRV for HA compared to LA in the free head movement condition (*mov*; $t(24.7) = -3.0$, $p = .007$), but not in the condition without head movement (*nomov*; $t(28.0) = -1.1$, $p = .285$).

We observed the same patterns for LF-HRV, that is, a significant main effect of arousal $F(1, 26.9) = 9.5$, $p = .005$; see Figure S1 in Supplements), no significant main effect of movement ($F(1, 25.5) = 2.2$, $p = .152$), and no significant arousal-by-movement interaction ($F(1, 26.0) = 0.5$, $p = .492$). Post-hoc pairwise comparisons of the estimated marginal means revealed significantly lower LF-HRV during higher arousal in the *mov* ($t(25.1) = -3.2$, $p = .004$), but not in the *nomov* ($t(28.0) = -1.6$, $p = .124$) condition.

No significant effects were observed on heart rate (i.e., IBI; all $p > .05$; see Figure S1 in Supplements).

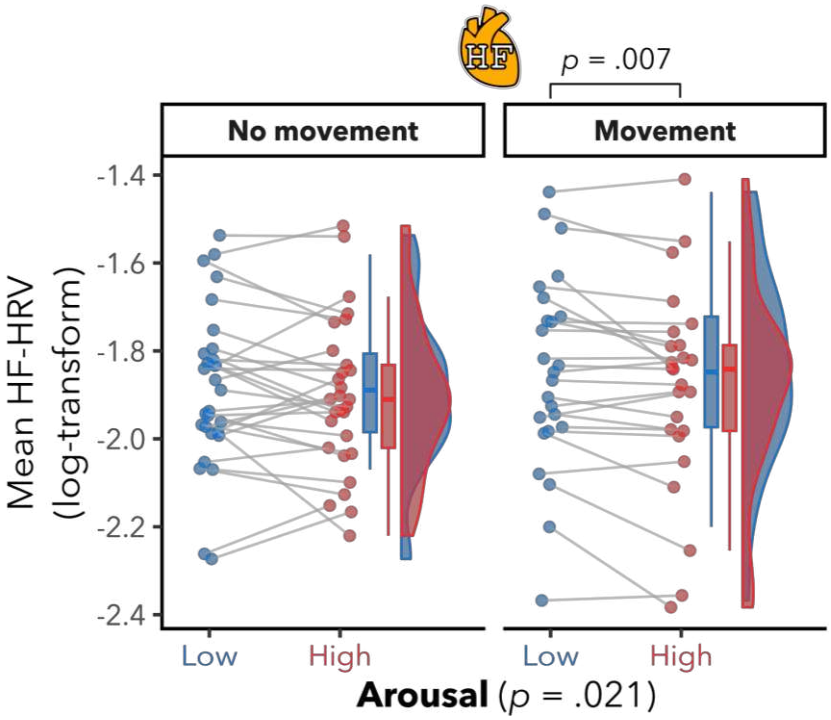

406

407 ***Figure 2.*** *Significant high-frequency heart rate variability (HF-HRV) differences between high*

408 *and low emotional arousal, in the free head movement condition. Mean HF-HRV per participant*

409 *for low (blue color) and high (red color) arousal and for runs without and with free head*

410 *movement. Box plots (horizontal bar: mean; whiskers: 1.5 interquartile range); individual dots*

411 *represent individual participants. There was a significant effect of arousal, but not of head*

412 *movement nor the interaction. Post-hoc pairwise comparisons showed lower HF-HRV during*

413 *higher arousal in the free head movement condition, but not in the without head movement*

414 *condition. There was no evidence for any significant effects of arousal, movement nor interaction*

415 *on interbeat intervals (IBI) (see Figure S1 in Supplements). There was also a significant effect of*

416 *arousal on LF-HRV (see Figure S1 in Supplements), but no significant effects of movement nor*

417 *interaction.*

3. Brain/EEG

We found a significant effect of arousal ($F(1, 27.7) = 30.7$, $p < .001$) on participants' alpha power in parieto-occipital regions (see Figure 3). There were no significant head movement ($F(1, 24.1) = 2.5$, $p = .128$) nor interaction effects ($F(1, 24.1) = 2.9$, $p = .101$). Post-hoc pairwise comparisons of the estimated marginal means revealed significantly lower alpha power in parieto-occipital regions for HA compared to LA in both the free (*mov*; $t(25.9) = -3.2$, $p = .004$) and without (*nomov*; $t(28.0) = -6.6$, $p < .001$) head movement conditions.

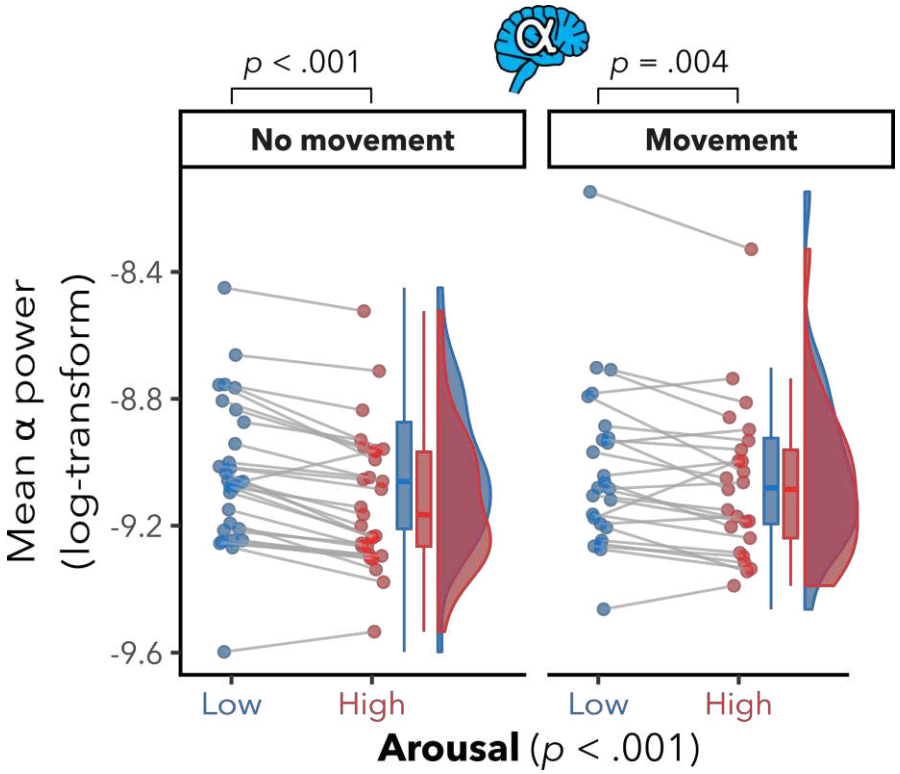

Figure 3. *Lower parieto-occipital alpha power in high vs. low arousal. Mean log α power within the region of interest (ROI: electrodes Pz, P3, P4, P7, P8, O1, O2, and Oz) per participant for low (blue color) and high (red color) arousal and for runs with and without free head movement. Box plots (horizontal bar: mean; whiskers: 1.5 interquartile range); individual dots represent individual participants. There were significant effects of arousal, but not of head movement nor*

interaction. Post-hoc pairwise comparisons showed significantly lower alpha power in parieto-occipital regions for HA compared to LA in both the free and without head movement conditions.

4. Brain-Heart

4.1. HEP

The cluster-based permutation tests revealed a significant HEP difference between HA and LA, indicated by a cluster at the left fronto-central regions (C3, FC1, FC5, Fz, F3 electrodes; Monte Carlo p = .019; see Figure 4A) from 328 to 360 ms after R-peak, with lower (i.e., more negative) HEP amplitude for HA than for LA (see Figure 4B).

The source localization (via eLORETA) yielded a distribution of sources where the strongest values were located close to and inside the central sulcus, in premotor, sensorimotor and supplementary motor areas (see Figure 4C).

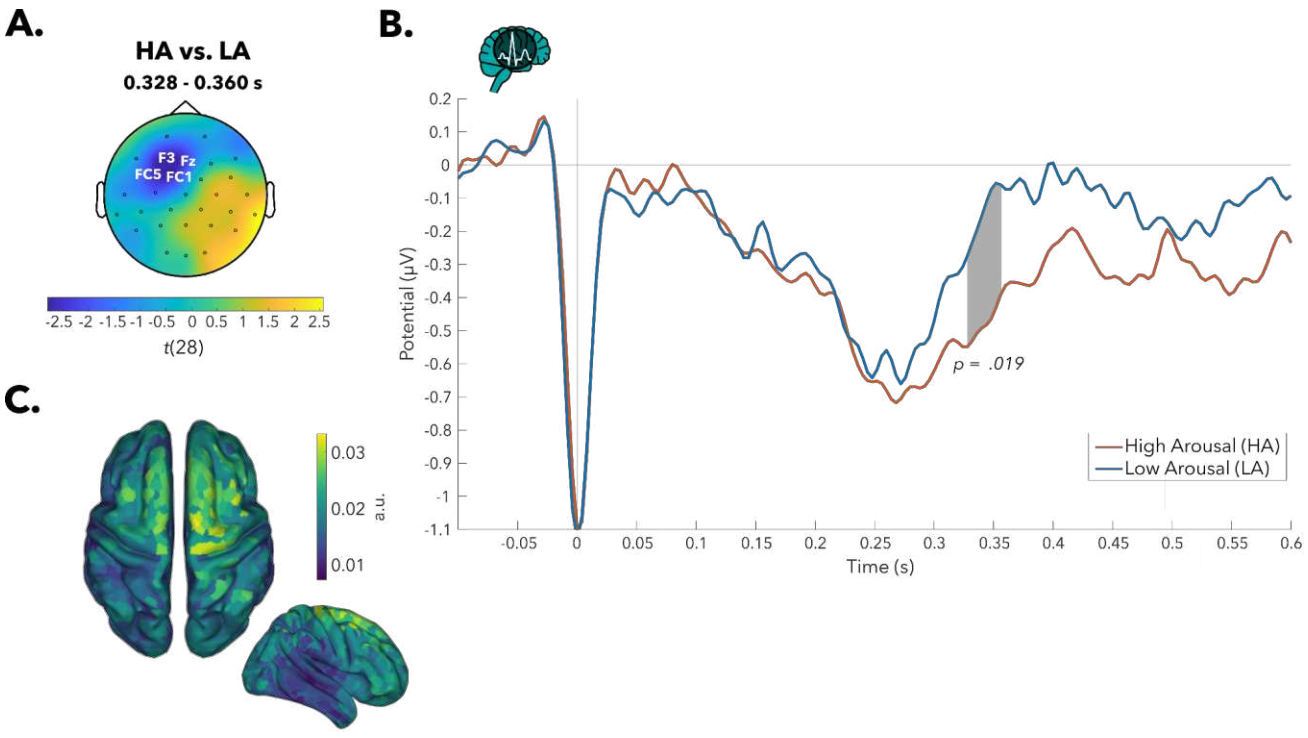

Figure 4. *Heartbeat-evoked potential (HEP) amplitudes significantly differed between high (HA) and low arousal (LA) over left fronto-central electrodes.* ***A.*** *Topographical map of t-values for HEP differences between HA and LA: Grand average across 29 participants (pooled data across both head movement conditions) in the 328- to 360-ms time window, where a significant difference (HA > LA) was observed in the cluster of highlighted electrodes.* ***B.*** *HEP time courses (HA in red, LA in blue) averaged across the cluster.* ***C.*** *Source localization (exact low resolution tomography analysis [eLORETA]) of HEP differences between HA and LA. The projection in source space suggests a distribution of sources with strongest values in premotor, sensorimotor, supplementary motor areas, around the central sulcus. Colors represent the inversely modeled contribution of the cortical voxels to the spatial pattern yielded by the HA vs. LA contrast.*

We also observed another cluster over right temporo-parietal electrodes (P8, TP10, T8 electrodes, from 352 to 356 ms after R-peak), with higher HEP amplitudes for HA compared to LA. This cluster, however, did not survive cluster-correction for multiple comparisons (Monte Carlo p = .310).

4.2. SDG

For an overview, the mean time-series over all participants of heart, brain and brain-heart metrics of interest, for the condition with free head movement (*mov*), are presented in Figure 5. The time-series for the condition without head movement (*nomov*) are available in the Supplements (see Figure S2).

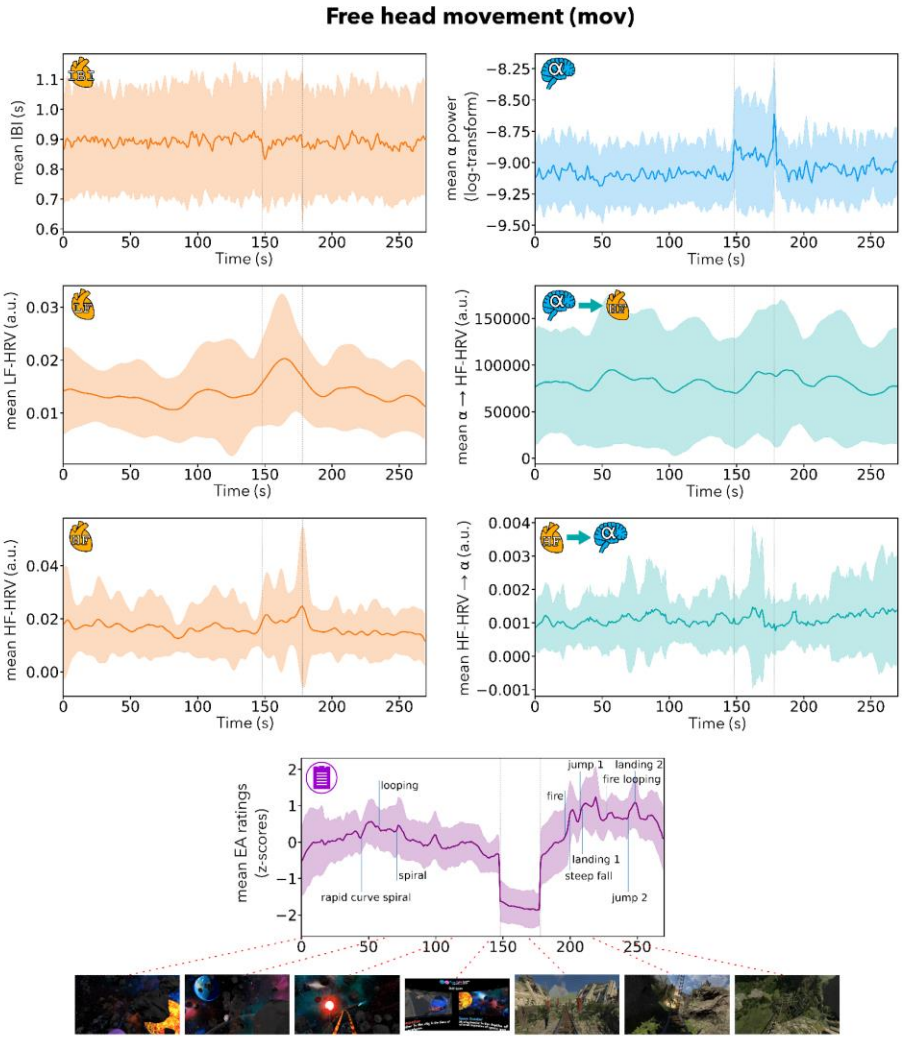

462

463 ***Figure 5.*** *Mean time-series across participants of interbeat intervals (IBI), low-frequency heart*
464 *rate variability (LF-HRV), high-frequency heart rate variability (HF-HRV), log α power averaged*
465 *across the region of interest (ROI: electrodes Pz, P3, P4, P7, P8, O1, O2, and Oz), brain-to-heart*
466 *coupling coefficient (α → HF-HRV; averaged across ROI), heart-to-brain coupling coefficient*
467 *(HF-HRV → α; averaged across ROI) and emotional arousal ratings, for the condition with free*
468 *head movement (mov). The shaded areas represent +/− 1 SD. Coloured lines: mean across*
469 *participants; vertical lines (light grey): beginning and end of the break; vertical lines (blue):*
470 *manually labeled salient events (for illustration). Bottom row: exemplary screenshots of the virtual*

reality (VR) experience. The time-series for the condition without head movement (nomov) are shown in the Supplements (see Figure S2).

There was no significant main effect of arousal (HF-HRV → α: $F(1, 27.1) = 0.01$, $p = .934$; α → HF-HRV: $F(1, 22.3) = 0.3$, $p = .619$) on the BHI coupling coefficients in both directions (see Figure 6). There was also no evidence for a main effect of movement (HF-HRV → α: $F(1, 24.3) = 0.8$, $p = .371$; α → HF-HRV: $F(1, 23.5) = 1.0$, $p = .339$) nor an arousal-by-movement interaction (HF-HRV → α: $F(1, 25.2) = 1.6$, $p = .217$; α → HF-HRV: $F(1, 22.7) = 0.01$, $p = .930$).

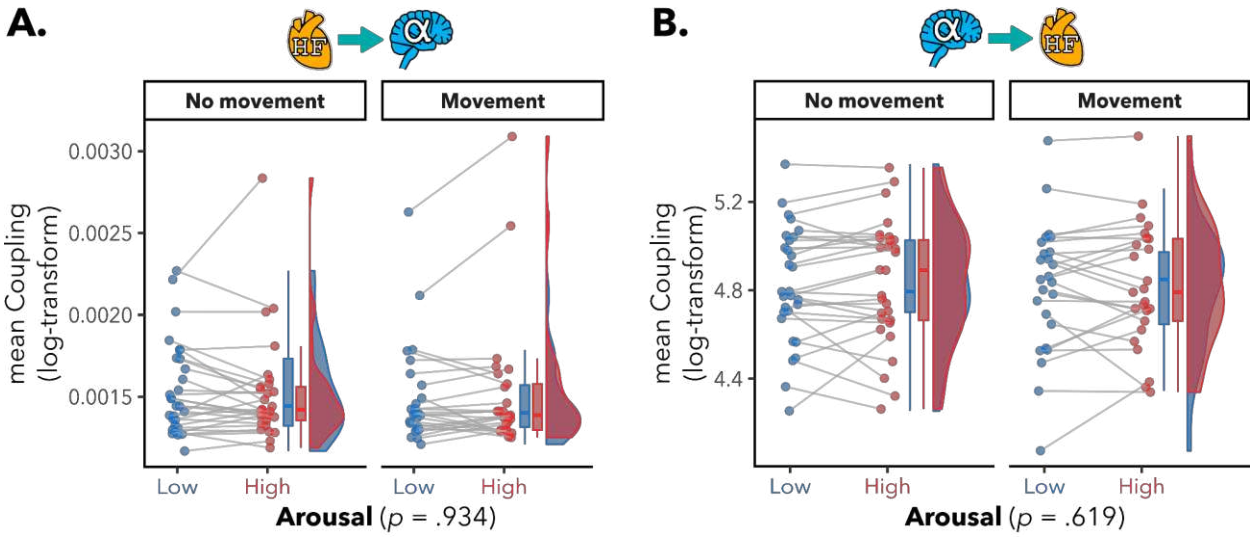

Figure 6. *No significant Brain-Heart Interaction (BHI) differences between high and low emotional arousal. Mean directional BHI coupling coefficients per participant, for low (blue color) and high (red color) arousal, and for runs with and without free head movement. The BHI coupling coefficients were computed using a Synthetic Data Generation (SDG) model (Catrambone et al., 2019); Heart related input: high-frequency heart rate variability (HF-HRV); Brain related input: α power within ROI. Box plots (horizontal bar: mean; whiskers: 1.5 interquartile range); individual dots represent individual participants.* ***A.*** *Heart-to-brain coupling coefficient (HF-HRV → α; averaged across ROI). There was no evidence for any significant effects*

*of arousal, movement nor interaction on HF-HRV → α (all $p > .05$). **B.** Brain-to-heart coupling coefficient (α → HF-HRV; averaged across ROI) during HA than LA. There was no evidence for any significant effects of arousal, movement nor interaction on α → HF-HRV (all $p > .05$).*

5. Control and Exploratory Analyses

5.1. ECG waveform

There were no significant differences (max $t(28) = 1.1$, min $p = .27$, FDR-corrected) in the ECG waveform between HA and LA conditions at all the time-points within the time window of EA related HEP differences (328 to 360 ms after R-peak).

5.2. Other frequency bands

A summary of the results can be found in Table 1 and figures including topographies in the Supplements.

Exploring arousal-related changes in whole-brain activity, we found different patterns of activation for HA vs. LA (see Figure S3 in Supplements). For the theta band, we found 17 EEG electrodes (see Table 1) with lower theta power during higher arousal. For the alpha band, there were 23 EEG electrodes with lower alpha power during higher arousal. For the beta band, there were 6 EEG electrodes with lower beta power during higher arousal. For the gamma band, one EEG electrode showed higher gamma power during higher arousal.

Exploring further arousal-related changes in BHI, we found different patterns of activation for HA vs. LA (see Figure S4 in Supplements). For HF-HRV → δ, one EEG electrode (see Table 1) showed lower BHI coupling coefficients during higher arousal. For LF-HRV → δ, one EEG electrode showed higher BHI coupling coefficients during higher arousal. For HF-HRV → α,

one EEG electrode showed lower BHI coupling coefficients during higher arousal. For HF-HRV → β, two EEG electrodes showed lower BHI coupling coefficients during higher arousal. For HF-HRV → γ, one EEG electrode showed higher BHI coupling coefficients during higher arousal. For LF-HRV → γ, there were 12 EEG electrodes (see Table 1) with higher BHI coupling coefficients during higher arousal. For γ → HF-HRV, there were 17 EEG electrodes with lower BHI coupling coefficients during higher arousal. Furthermore, concerning the gamma band, when looking at the interception (FC5, CP5, P3, T7, TP9, TP10, O1, Oz, O2) of both significant electrodes for the ascending (LF-HRV → γ) and descending (γ → HF-HRV) directions, both effects were still present (LF-HRV → γ: $t(28) = 2.8$; $p = .008$; γ → HF-HRV: $t(28) = -2.7$; $p = .012$).

518

HA vs. LA	direction effect	electrodes with significant differences ($p_{uncorrected}$ < .05 and $\boldsymbol{p_{FDR}}$ **< .05**)
Brain/EEG		
θ (4–8 Hz)	HA < LA	Fp1, **Fp2**, Fz, F3, FC1, **FC2**, FC6, C3, **C4**, CP1, CP5, P4, P7, **TP9**, TP10, O1, O2
α (8–13 Hz)	HA < LA	**Fp1, Fp2, Fz, F3, F4, FC1, FC2, FC6, Cz, C4, CP1, CP5, CP6, Pz**, **P3, P4, P7, P8, TP9, TP10, T8, O1, O2**
β (13–30 Hz)	HA < LA	FC2, C4, **CP1, Pz, P3, P4**
γ (30–45 Hz)	HA > LA	O2
Brain-Heart (SDG)		
Ascending		
LF-HRV → δ	HA > LA	P8
LF-HRV → γ	HA > LA	Fp2, Fz, FC5, CP5, P3, P8, T7, TP9, TP10, Oz, O1, O2
HF-HRV → δ	HA < LA	O1
HF-HRV → α	HA < LA	**P3**
HF-HRV → β	HA < LA	Pz, CP2
HF-HRV → γ	HA > LA	O2
Descending		
γ → HF-HRV	HA < LA	Fp1, F3, FC5, FC6, C3, CP5, CP6, P3, P4, P7, T7, T8, TP9, TP10, Oz, O1, O2

519 ***Table 1.*** *Summary of the exploratory analyses. At each electrode, the different metrics were*
520 *averaged over the head movement conditions, and paired t-tests were performed between the mean*
521 *during high arousal (HA) and the mean during low arousal (LA) for each participant.*
522 *Topographies can be found in the Supplements (see Figure S3 and S4). SDG: synthetic data*
523 *generation modeling; LF/HF-HRV: low/high-frequency heart rate variability.*

Discussion

We investigated brain-heart interactions during an emotionally arousing experience in immersive VR. In particular, we analyzed EA-related cardiac activity (particularly its vagal regulation) and the extent to which it contributed to the previously reported link between EA and parieto-occipital alpha power (Hofmann, Klotzsche, Mariola et al., 2021). We found differences in heart activity, brain activity and - less consistently - brain-heart interactions between states of HA and LA. More specifically, we observed significant arousal-related BHI differences in event-related analyses (i.e., HEPs) but not in oscillatory analyses (i.e., SDG modeling), although whole-brain exploratory analyses pointed towards increased ascending heart-to-brain (i.e., LF-HRV → γ) and reduced descending brain-to-heart (i.e., γ → HF-HRV) functional information flow during higher EA. Generally, our findings extend previous results from classical studies and confirm the link between EA and HF-HRV, parieto-occipital alpha power, and HEP amplitude under more naturalistic conditions.

1. Heart/ECG

Analyzing the heart signal, we found significant effects of EA on both LF- and HF-HRV. This is in line with previous research showing lower HF-HRV during states of higher EA (Valenza et al., 2012; Luft & Bhattacharya, 2015; Hildebrandt et al., 2016). As HF-HRV reflects vagal cardioregulation (Task Force, 1996), a possible interpretation is that the parasympathetic regulation of heart activity decreased (i.e., vagal withdrawal) during higher EA. Fluctuations in HF-HRV during emotion have been associated with functional changes in medial prefrontal cortex (Lane et al., 2009), a brain region shared by the CAN and the SN. The changes in HF-HRV during

EA could therefore be also linked to a (bottom-up) modulation of attention in presence of emotional stimuli.

Concerning LF-HRV, the measure reflects both the sympathetic and parasympathetic influences on the heart rate. While the EA-related changes in LF-HRV could thus be driven by changes in parasympathetic activity, it remains unclear why we did not find evidence for heart rate differences between LA and HA. As both ANS branches can be active at the same time (Koizumi et al., 1983; Paton et al., 2005), their contribution to the heart rate may have canceled each other out (to only be visible in the variability measures LF- and HF-HRV). Because the heart rate and its sympathetic regulation are known to change more slowly (order of few seconds) than its parasympathetic regulation (order of ms), it is also possible that our analysis (with 1 s resolution) did not capture these delayed changes. Future studies may consider directly assessing the sympathetic regulation of the heart and its potential link to emotional arousal, for instance by modeling regulations at different timescales to extract a sympathetic activity index (Valenza et al., 2018) from the ECG signal and take into account the potential delay of the sympathetic regulation.

2. Brain/EEG

Analyzing the brain activity, we confirmed our previous findings of lower parieto-occipital alpha power for HA compared to LA states (Hofmann, Klotzsche, Mariola et al., 2021) with a different statistical approach, using LMM instead of decoding. Of note, exploratory analyses suggest that this effect is not restricted to parieto-occipital cortical areas. This is also in line with previous research using event-related designs (Koelstra et al., 2012; Luft & Bhattacharya, 2015). Because alpha power has also been linked to attentional processes (Klimesch, 2012; van Diepen et al., 2019) and to the encoding of the emotional salience of stimuli (e.g., in orbitofrontal cortex; Todd et al., 2014), the change in alpha power might indicate a (bottom-up) modulation of attention in presence

of emotional stimuli (Sutherland & Mather, 2018) - which may be present with a more widespread topography.

In additional exploratory analyses, we investigated EA-related differences in other frequency bands. We observed significant effects in other frequency bands, such as lower theta power (cf. Aftanas et al., 2002), lower beta power (Schubring et al., 2020; Kim et al., 2021), and higher gamma power (Cao et al., 2020) during HA vs. LA, but these findings should be interpreted with caution given the exploratory nature of these analyses and the risk of false positives.

The main aim of this work was to investigate if these changes in parieto-occipital alpha oscillations and the changes we observed in heart activity (i.e., in HF-HRV) were related to each other. Given the alpha reduction during HA compared to LA, how did vagal cardioregulation come into play?

3. Brain-Heart

Combining heart and brain activities together in a multimodal analysis, we investigated BHI during different states of emotional arousal. Using two different approaches, an event-related and an oscillatory analysis, we found - though not consistently across both approaches - that the functional coupling between the heart and the brain was linked to emotional arousal.

Looking at HEPs (event-related analysis), we found a significantly lower (or more negative) HEP amplitude for high compared to low arousal in left fronto-central electrodes. Because there was no significant difference in heart rate (i.e., IBIs) nor in ECG waveform between HA and LA, this HEP difference may not be due to residual CFA nor to a difference of duration between heartbeats. We did not replicate the findings from Luft & Battacharya (2015), in that we did not find a significantly higher HEP amplitude in parieto-occipital regions during higher arousal (a pattern, which we only observed in a non-significant cluster). The topography of the fronto-central cluster, however, might reflect the anterior pole of a dipole that is also visible at the parietal electrodes. Particularly, a

separation with an angle of approximately 45° between the positive and negative pole on the scalp is often characteristic of a tangential equivalent dipolar source located inside the central sulcus (e.g., for the somatosensory evoked potential N20; Scherg et al., 2019). Our source localization results support this view by pointing towards a distribution of sources around the central sulcus, in sensorimotor areas. The left fronto-central topography observed here and the right parieto-occipital topography reported by Luft and Battacharya (2015) may thus reflect similar underlying sources.

Our HEP results are also in line with a meta-analysis (Coll et al., 2021) that found a large effect of arousal (including but not restricted to *emotional* arousal) on HEP amplitudes, with the strongest effect around 250 ms after R-peak and in fronto-central electrodes (Cz, C1, C2, C3, C4, FCz, FC1, FC2, FC3, FC4, FC5, FC6 and AFz). More specifically related to *emotional* arousal, a recent study (Marshall et al., 2019) included in this meta-analysis found a HEP suppression for angry vs. neutral faces when they were repeatedly presented. This could reflect a different weighing of exteroceptive vs. interoceptive information to facilitate rapid perceptual processing and behavioral responses, as well as to mobilize (e.g., metabolic) resources (Gianaros & Wager, 2015).

In the confirmatory oscillatory analysis using SDG modeling, we did not find evidence for an association between EA and directional communication between the brain (indexed by parieto-occipital alpha power) and the heart (indexed by HF-HRV). The results of the SDG whole-scalp exploratory analysis of multiple frequency bands indicated that EA was associated with specific changes in information flow from the heart to the brain (higher LF-HRV → γ in a temporo-occipital cluster, lower information flow from HF-HRV to the brain in single electrodes) and - less so - from the brain to the heart (lower γ → HF-HRV in a temporo-occipital cluster; Table 1 for details). Although this should, again, be interpreted with caution, these results suggest a link

between the level of EA and the coupling between HRV and brain activity in different frequency bands. Particularly, ascending signals of heart activity seem to inform brain activity and modulate the emotional experience (Candia-Rivera et al., 2022). Our results are partly consistent with the findings of Candia-Rivera and colleagues (2022), who reported higher (ascending) heart-to-brain information flow - although in different frequency bands - during higher arousal, and lower (descending) brain-to-heart information flow during emotion elicitation compared to rest. Interestingly, genetically modified mice with chronically elevated heart rate (within the physiological range) had higher HF-HRV, higher EEG gamma band power, and higher ascending information flow from LF-HRV to gamma compared to control mice (Agrimi et al., 2023).

Overall, these results extend our previous contribution to the physiology of emotional experience using immersive VR, with our previous "brain-only" results of EEG-derived parieto-occipital alpha power (Hofmann, Klotzsche, Mariola et al., 2021) now complemented by considering the rest of the body (here: the heart or ANS). During states of higher emotional arousal, not only parieto-occipital alpha power was lower but so were LF-HRV, HF-HRV, and HEP amplitudes over fronto-central electrodes. While we did not find evidence for the hypothesized changes in BHI between parieto-occipital alpha power and HF-HRV (in either direction), exploratory analyses suggest several other EA-related BHI changes, notably in temporo-occipital gamma power, where higher EA was linked to decreased brain-to-heart ($\gamma \rightarrow$ HF-HRV) and increased heart-to-brain (LF-HRV $\rightarrow \gamma$) information flow. Thereby, heart-to-brain information flow seems to change more broadly (in time and space) with different affective states than - in the opposite direction - the brain-to-heart information flow. This supports the view that signals from the internal body (e.g., the heart) influence our perception of the world and our interaction with it (Ohl et al., 2016; Kunzendorf et al., 2019; Motyka et al., 2019; Galvez-Pol et al., 2022). Changes in bodily

637 rhythms, as they occur in different affective states, change attentional processes (Sutherland &
638 Mather, 2018) or - more generally - the way in which sensory evidence is accumulated (Allen et
639 al., 2022), for example through increased ascending (heart-to-brain) compared to reduced
640 descending (brain-to-heart) information flow.

641 ## 4. Limitations and Future Directions

642 Several limitations should be considered when interpreting our findings. While the dataset is
643 relatively short and potentially noisy due to the more naturalistic conditions of data acquisition,
644 this is a tradeoff that comes with using a more realistic affective stimulation.
645 Other limitations are due to the approach of a secondary analysis - the experimental design was
646 not optimized for some analysis methods used here. For example, to avoid transition effects
647 between the different parts of the VR experience, data needed to be trimmed at the beginning and
648 end of rollercoasters. This discontinuity was not ideal for time-resolved metrics such as heart rate,
649 HRV and SDG couplings. Fully continuous data without trimming would be preferable in future
650 experiments.
651 Furthermore, the EA ratings were binned into HA and LA in order to increase sensitivity and to
652 maximize comparability to previous findings (Luft & Bhattacharya, 2015) as well as our previous
653 analyses (Hofmann, Klotzsche, Mariola et al., 2021). Models that include the continuous ratings
654 (as also part of Hofmann, Klotzsche, Mariola et al., 2021) can provide a more fine-grained picture
655 of the relationship between emotional arousal and physiological measures.
656 As respiration modulates vagal cardioregulation (Benarroch, 1993) and HEP amplitudes (Zaccaro
657 et al., 2022), we cannot exclude potential EA-related changes in respiration (e.g., its rate) and
658 assess their influence on measures of BHI. In the future, respiratory activity should also be added
659 to the physiological measurements of BHI studies (e.g., with a respiration belt).

660 Finally, the inclusion of (e.g., behavioral or eye movement-related) measures of attention could
661 support the interpretation of emotion-related modulations of attention (as reflected in changes in
662 vagal cardioregulation and parieto-occipital alpha power).

Conclusion

We replicated previous findings from classical studies in a more naturalistic virtual reality setting, confirming the link between emotional arousal, heart activity, brain oscillations and - albeit less consistently - brain-heart interactions. Our analysis demonstrates that combining measures of heart and brain activity provides insights beyond what can be learned from studying each modality in isolation. Finally, this work illustrates how VR paired with multimodal physiological recordings can be a valuable approach for simultaneously studying multiple components of emotions. Taken together, our results suggest that to better understand affective processes, we must consider the heart alongside the brain, as both play integral roles in emotion.

References

Aftanas, L. I., Varlamov, A. A., Pavlov, S. V., Makhnev, V. P., & Reva, N. V. (2002). Time-dependent cortical asymmetries induced by emotional arousal: EEG analysis of event-related synchronization and desynchronization in individually defined frequency bands. *International Journal of Psychophysiology*, *44*(1), 67–82. https://doi.org/10.1016/S0167-8760(01)00194-5

Agrimi, J., Menicucci, D., Qu, J.-H., Laurino, M., Mackey, C. D., Hasnain, L., Tarasova, Y. S., Tarasov, K. V., McDevitt, R. A., Hoover, D. B., Gemignani, A., Paolocci, N., & Lakatta, E. G. (2023). Enhanced Myocardial Adenylyl Cyclase Activity Alters Heart-Brain Communication. *JACC: Clinical Electrophysiology*, *9*(11), 2219–2235. https://doi.org/10.1016/j.jacep.2023.07.023

Al, E., Iliopoulos, F., Forschack, N., Nierhaus, T., Grund, M., Motyka, P., Gaebler, M., Nikulin, V. V., & Villringer, A. (2020). Heart–brain interactions shape somatosensory perception and evoked potentials. Proceedings of the National Academy of Sciences, 117(19), Article 19. https://doi.org/10.1073/pnas.1915629117

Allen, M., Levy, A., Parr, T., & Friston, K. J. (2022). In the Body's Eye: The computational anatomy of interoceptive inference. PLOS Computational Biology, 18(9), e1010490. https://doi.org/10.1371/journal.pcbi.1010490

Al-Nashash, H., Al-Assaf, Y., Paul, J., & Thakor, N. (2004). EEG signal modeling using adaptive Markov process amplitude. IEEE Transactions on Biomedical Engineering, 51(5), 744–751. https://doi.org/10.1109/TBME.2004.826602

Babloyantz, A., & Destexhe, A. (1988). Is the normal heart a periodic oscillator? Biological Cybernetics, 58(3), 203–211. https://doi.org/10.1007/BF00364139

Barr, D. J., Levy, R., Scheepers, C., & Tily, H. J. (2013). Random effects structure for confirmatory hypothesis testing: Keep it maximal. Journal of Memory and Language, 68(3), 10.1016/j.jml.2012.11.001. https://doi.org/10.1016/j.jml.2012.11.001

Barrett, L. F. (2016). The theory of constructed emotion: An active inference account of interoception and categorization. Social Cognitive and Affective Neuroscience, nsw154. https://doi.org/10.1093/scan/nsw154

Barrett, L. F., & Russell, J. A. (1999). The Structure of Current Affect: Controversies and Emerging Consensus. Current Directions in Psychological Science, 8(1), 10–14. https://doi.org/10.1111/1467-8721.00003

Bates, D., Mächler, M., Bolker, B., & Walker, S. (2014). Fitting Linear Mixed-Effects Models using lme4 (arXiv:1406.5823). arXiv. https://doi.org/10.48550/arXiv.1406.5823

Baumgartner, T., Valko, L., Esslen, M., & Jäncke, L. (2006). Neural Correlate of Spatial Presence in an Arousing and Noninteractive Virtual Reality: An EEG and Psychophysiology Study. CyberPsychology & Behavior, 9(1), 30–45. https://doi.org/10.1089/cpb.2006.9.30

Benarroch, E. E. (1993). The Central Autonomic Network: Functional Organization, Dysfunction, and Perspective. Mayo Clinic Proceedings, 68(10), 988–1001. https://doi.org/10.1016/S0025-6196(12)62272-1

Benjamini, Y., & Yekutieli, D. (2001). The Control of the False Discovery Rate in Multiple Testing under Dependency. The Annals of Statistics, 29(4), 1165–1188.

Berger, H. (1929). Über das Elektrenkephalogramm des Menschen. Archiv für Psychiatrie und Nervenkrankheiten, 87(1), 527–570. https://doi.org/10.1007/BF01797193

Bigdely-Shamlo, N., Mullen, T., Kothe, C., Su, K.-M., & Robbins, K. A. (2015). The PREP pipeline: Standardized preprocessing for large-scale EEG analysis. Frontiers in Neuroinformatics, 9. https://www.frontiersin.org/article/10.3389/fninf.2015.00016

Bohil, C. J., Alicea, B., & Biocca, F. A. (2011). Virtual reality in neuroscience research and therapy. Nature Reviews Neuroscience, 12(12), Article 12. https://doi.org/10.1038/nrn3122

Brennan, M., Palaniswami, M., & Kamen, P. (2002). Poincaré plot interpretation using a physiological model of HRV based on a network of oscillators. American Journal of Physiology-Heart and Circulatory Physiology, 283(5), H1873–H1886. https://doi.org/10.1152/ajpheart.00405.2000

Bridwell, D. A., Cavanagh, J. F., Collins, A. G. E., Nunez, M. D., Srinivasan, R., Stober, S., & Calhoun, V. D. (2018). Moving Beyond ERP Components: A Selective Review of Approaches to Integrate EEG and Behavior. Frontiers in Human Neuroscience, 12. https://www.frontiersin.org/articles/10.3389/fnhum.2018.00106

Buzsaki, G. (2006). Rhythms of the Brain. Oxford University Press.

Buzsáki, G., Logothetis, N., & Singer, W. (2013). Scaling Brain Size, Keeping Timing: Evolutionary Preservation of Brain Rhythms. Neuron, 80(3), 751–764. https://doi.org/10.1016/j.neuron.2013.10.002

Candia-Rivera, D., Catrambone, V., Thayer, J. F., Gentili, C., & Valenza, G. (2022). Cardiac sympathetic-vagal activity initiates a functional brain–body response to emotional arousal. Proceedings of the National Academy of Sciences, 119(21), e2119599119. https://doi.org/10.1073/pnas.2119599119

Cao, R., Shi, H., Wang, X., Huo, S., Hao, Y., Wang, B., Guo, H., & Xiang, J. (2020). Hemispheric Asymmetry of Functional Brain Networks under Different Emotions Using EEG Data. Entropy, 22(9), Article 9. https://doi.org/10.3390/e22090939

Catrambone, V., Greco, A., Vanello, N., Scilingo, E. P., & Valenza, G. (2019). Time-Resolved Directional Brain–Heart Interplay Measurement Through Synthetic Data Generation Models. Annals of Biomedical Engineering, 47(6), Article 6. https://doi.org/10.1007/s10439-019-02251-y

Chaumon, M., Bishop, D. V. M., & Busch, N. A. (2015). A practical guide to the selection of independent components of the electroencephalogram for artifact correction. Journal of Neuroscience Methods, 250, 47–63. https://doi.org/10.1016/j.jneumeth.2015.02.025

Coll, M.-P., Hobson, H., Bird, G., & Murphy, J. (2021). Systematic review and meta-analysis of the relationship between the heartbeat-evoked potential and interoception. Neuroscience & Biobehavioral Reviews, 122, 190–200. https://doi.org/10.1016/j.neubiorev.2020.12.012

Craig, A. D. (2002). How do you feel? Interoception: The sense of the physiological condition of the body. Nature Reviews Neuroscience, 3(8), 655–666. https://doi.org/10.1038/nrn894

Craig, A. D. (2009). How do you feel — now? The anterior insula and human awareness. Nature Reviews Neuroscience, 10(1), Article 1. https://doi.org/10.1038/nrn2555

Dalgleish, T. (2004). The emotional brain. Nature Reviews Neuroscience, 5(7), Article 7. https://doi.org/10.1038/nrn1432

Delorme, A., & Makeig, S. (2004). EEGLAB: An open source toolbox for analysis of single-trial EEG dynamics including independent component analysis. Journal of Neuroscience Methods, 134(1), 9–21. https://doi.org/10.1016/j.jneumeth.2003.10.009

Diemer, J., Alpers, G. W., Peperkorn, H. M., Shiban, Y., & Mühlberger, A. (2015). The impact of perception and presence on emotional reactions: A review of research in virtual reality. Frontiers in Psychology, 6. https://doi.org/10.3389/fpsyg.2015.00026

Dores, A. R., Barbosa, F., Monteiro, L., Reis, M., Coelho, C. M., Ribeiro, E., Leitão, M., Carvalho, I. P., de Sousa, L., & Castro-Caldas, A. (2014). Amygdala activation in response to 2D and 3D emotion-inducing stimuli. PsychNology Journal, 12, 29–43.

Driver, J. (2001). A selective review of selective attention research from the past century. British Journal of Psychology, 92(1), 53–78. https://doi.org/10.1348/000712601162103

Dusi, V., & Ardell, J. L. (2020). Brain-Heart Afferent-Efferent Traffic. In S. Govoni, P. Politi, & E. Vanoli (Eds.), Brain and Heart Dynamics (pp. 1–23). Springer International Publishing. https://doi.org/10.1007/978-3-319-90305-7_2-1

Egeth, H. E., & Yantis, S. (1997). VISUAL ATTENTION: Control, Representation, and Time Course. Annual Review of Psychology, 48(1), 269–297. https://doi.org/10.1146/annurev.psych.48.1.269

Galvez-Pol, A., Virdee, P., Villacampa, J., & Kilner, J. (2022). Active tactile discrimination is coupled with and modulated by the cardiac cycle. eLife, 11, e78126. https://doi.org/10.7554/eLife.78126

García-Cordero, I., Esteves, S., Mikulan, E. P., Hesse, E., Baglivo, F. H., Silva, W., García, M. del C., Vaucheret, E., Ciraolo, C., García, H. S., Adolfi, F., Pietto, M., Herrera, E., Legaz, A., Manes, F., García, A. M., Sigman, M., Bekinschtein, T. A., Ibáñez, A., & Sedeño, L. (2017). Attention, in and Out: Scalp-Level and Intracranial EEG Correlates of Interoception and Exteroception. Frontiers in Neuroscience, 11. https://www.frontiersin.org/articles/10.3389/fnins.2017.00411

Gehrlach, D. A., Dolensek, N., Klein, A. S., Roy Chowdhury, R., Matthys, A., Junghänel, M., Gaitanos, T. N., Podgornik, A., Black, T. D., Reddy Vaka, N., Conzelmann, K.-K., & Gogolla, N. (2019). Aversive state processing in the posterior insular cortex. Nature Neuroscience, 22(9), Article 9. https://doi.org/10.1038/s41593-019-0469-1

Gianaros, P. J., & Wager, T. D. (2015). Brain-Body Pathways Linking Psychological Stress and Physical Health. Current Directions in Psychological Science, 24(4), 313–321. https://doi.org/10.1177/0963721415581476

Goldstein, D. S., Bentho, O., Park, M.-Y., & Sharabi, Y. (2011). Low-frequency power of heart rate variability is not a measure of cardiac sympathetic tone but may be a measure of modulation of cardiac autonomic outflows by baroreflexes. Experimental Physiology, 96(12), 1255–1261. https://doi.org/10.1113/expphysiol.2010.056259

Gramfort, A., Luessi, M., Larson, E., Engemann, D., Strohmeier, D., Brodbeck, C., Goj, R., Jas, M., Brooks, T., Parkkonen, L., & Hämäläinen, M. (2013). MEG and EEG data analysis with MNE-Python. Frontiers in Neuroscience, 7. https://www.frontiersin.org/article/10.3389/fnins.2013.00267

Greiner, B. (2015). Subject pool recruitment procedures: Organizing experiments with ORSEE. Journal of the Economic Science Association, 1(1), 114–125. https://doi.org/10.1007/s40881-015-0004-4

Gross, J. J. (1998). The Emerging Field of Emotion Regulation: An Integrative Review. Review of General Psychology, 2(3), 271–299. https://doi.org/10.1037/1089-2680.2.3.271

Grosse Rueschkamp, J. M., Brose, A., Villringer, A., & Gaebler, M. (2019). Neural correlates of up-regulating positive emotions in fMRI and their link to affect in daily life. Social Cognitive and Affective Neuroscience, 14(10), 1049–1059.

https://doi.org/10.1093/scan/nsz079

Haufe, S., & Ewald, A. (2019). A Simulation Framework for Benchmarking EEG-Based Brain Connectivity Estimation Methodologies. Brain Topography, 32(4), 625–642. https://doi.org/10.1007/s10548-016-0498-y

Haufe, S., Meinecke, F., Görgen, K., Dähne, S., Haynes, J.-D., Blankertz, B., & Bießmann, F. (2014). On the interpretation of weight vectors of linear models in multivariate neuroimaging. NeuroImage, 87, 96–110. https://doi.org/10.1016/j.neuroimage.2013.10.067

He, B. J. (2014). Scale-free brain activity: Past, present, and future. Trends in Cognitive Sciences, 18(9), 480–487. https://doi.org/10.1016/j.tics.2014.04.003

Hildebrandt, L. K., McCall, C., Engen, H. G., & Singer, T. (2016). Cognitive flexibility, heart rate variability, and resilience predict fine-grained regulation of arousal during prolonged threat. Psychophysiology, 53(6), 880–890. https://doi.org/10.1111/psyp.12632

Hofmann, S. M., Klotzsche, F., Mariola, A., Nikulin, V., Villringer, A., & Gaebler, M. (2021). Decoding subjective emotional arousal from eeg during an immersive virtual reality experience. eLife, 10, e64812. https://doi.org/10.7554/eLife.64812

Hsueh, B., Chen, R., Jo, Y., Tang, D., Raffiee, M., Kim, Y. S., Inoue, M., Randles, S., Ramakrishnan, C., Patel, S., Kim, D. K., Liu, T. X., Kim, S. H., Tan, L., Mortazavi, L., Cordero, A., Shi, J., Zhao, M., Ho, T. T., … Deisseroth, K. (2023). Cardiogenic control of affective behavioural state. Nature, 615(7951), Article 7951. https://doi.org/10.1038/s41586-023-05748-8

Huang, Y., Parra, L. C., & Haufe, S. (2016). The New York Head—A precise standardized volume conductor model for EEG source localization and tES targeting. NeuroImage, 140, 150–162. https://doi.org/10.1016/j.neuroimage.2015.12.019

Huk, A., Bonnen, K., & He, B. J. (2018). Beyond Trial-Based Paradigms: Continuous Behavior, Ongoing Neural Activity, and Natural Stimuli. Journal of Neuroscience, 38(35), 7551–7558. https://doi.org/10.1523/JNEUROSCI.1920-17.2018

Idaji, M. J., Müller, K.-R., Nolte, G., Maess, B., Villringer, A., & Nikulin, V. V. (2020). Nonlinear interaction decomposition (NID): A method for separation of cross-frequency coupled sources in human brain. NeuroImage, 211, 116599. https://doi.org/10.1016/j.neuroimage.2020.116599

James, W. (1884). II.—WHAT IS AN EMOTION? Mind, os-IX(34), 188–205. https://doi.org/10.1093/mind/os-IX.34.188

Kim, H., Seo, P., Choi, J. W., & Kim, K. H. (2021). Emotional arousal due to video stimuli reduces

local and inter-regional synchronization of oscillatory cortical activities in alpha- and beta-bands. PLoS ONE, 16(7), e0255032. https://doi.org/10.1371/journal.pone.0255032

Klein, A. S., Dolensek, N., Weiand, C., & Gogolla, N. (2021). Fear balance is maintained by bodily feedback to the insular cortex in mice. Science, 374(6570), 1010–1015. https://doi.org/10.1126/science.abj8817

Klimesch, W. (2012). Alpha-band oscillations, attention, and controlled access to stored information. Trends in Cognitive Sciences, 16(12), 606–617. https://doi.org/10.1016/j.tics.2012.10.007

Koelstra, S., Muhl, C., Soleymani, M., Lee, J., Yazdani, A., Ebrahimi, T., Pun, T., Nijholt, A., & Patras, I. (2012). DEAP: A Database for Emotion Analysis using Physiological Signals. IEEE Transactions on Affective Computing, 3(1), 18–31. https://doi.org/10.1109/T-AFFC.2011.15

Koizumi, K., Terui, N., & Kollai, M. (1983). Neural control of the heart: Significance of double innervation re-examined. Journal of the Autonomic Nervous System, 7(3), 279–294. https://doi.org/10.1016/0165-1838(83)90081-4

Kreibig, S. D. (2010). Autonomic nervous system activity in emotion: A review. Biological Psychology, 84(3), 394–421. https://doi.org/10.1016/j.biopsycho.2010.03.010

Kunzendorf, S., Klotzsche, F., Akbal, M., Villringer, A., Ohl, S., & Gaebler, M. (2019). Active information sampling varies across the cardiac cycle. Psychophysiology, 56(5), e13322. https://doi.org/10.1111/psyp.13322

Kuppens, P., Oravecz, Z., & Tuerlinckx, F. (2010). Feelings change: Accounting for individual differences in the temporal dynamics of affect. Journal of Personality and Social Psychology, 99(6), 1042–1060. https://doi.org/10.1037/a0020962

Kuznetsova, A., Brockhoff, P. B., & Christensen, R. H. B. (2017). lmerTest Package: Tests in Linear Mixed Effects Models. Journal of Statistical Software, 82, 1–26. https://doi.org/10.18637/jss.v082.i13

Lane, R. D., McRae, K., Reiman, E. M., Chen, K., Ahern, G. L., & Thayer, J. F. (2009). Neural correlates of heart rate variability during emotion. NeuroImage, 44(1), 213–222. https://doi.org/10.1016/j.neuroimage.2008.07.056

Lange, C. G. (1885). THE MECHANISM OF THE EMOTIONS. 8.

Larson, E., Gramfort, A., Engemann, D. A., Leppakangas, J., Brodbeck, C., Jas, M., Brooks, T., Sassenhagen, J., Luessi, M., King, J.-R., McCloy, D., Goj, R., Favelier, G., Höchenberger, R., Brunner, C., van Vliet, M., Wronkiewicz, M., Holdgraf, C., Massich, J., … buildqa. (2022). MNE-Python (1.1.0) [Computer software]. Zenodo.

Lee, T.-W., Girolami, M., & Sejnowski, T. J. (1999). Independent Component Analysis Using an Extended Infomax Algorithm for Mixed Subgaussian and Supergaussian Sources. Neural Computation, 11(2), 417–441. https://doi.org/10.1162/089976699300016719

Levy, M. N. (1971). Sympathetic-parasympathetic interactions in the heart. Circulation Research, 29(5), 437–445. https://doi.org/10.1161/01.res.29.5.437

Levy, M. N., & Martin, P. J. (1984). Neural Control of the Heart. In N. Sperelakis (Ed.), Physiology and Pathophysiology of the Heart (pp. 337–354). Springer US. https://doi.org/10.1007/978-1-4757-1171-4_15

Lindquist, K. A., Wager, T. D., Kober, H., Bliss-Moreau, E., & Barrett, L. F. (2012). The brain basis of emotion: A meta-analytic review. Behavioral and Brain Sciences, 35(03), 121–143. https://doi.org/10.1017/S0140525X11000446

Luft, C. D. B., & Bhattacharya, J. (2015). Aroused with heart: Modulation of heartbeat evoked potential by arousal induction and its oscillatory correlates. Scientific Reports, 5(1), Article 1. https://doi.org/10.1038/srep15717

Makowski, D., Pham, T., Lau, Z. J., Brammer, J. C., Lespinasse, F., Pham, H., Schölzel, C., & Chen, S. H. A. (2021). NeuroKit2: A Python toolbox for neurophysiological signal processing. Behavior Research Methods, 53(4), 1689–1696. https://doi.org/10.3758/s13428-020-01516-y

Marshall, A. C., Gentsch, A., & Schütz-Bosbach, S. (2019). Interoceptive cardiac expectations to emotional stimuli predict visual perception. Emotion, 20(7), 1113. https://doi.org/10.1037/emo0000631

Mauss, I. B., & Robinson, M. D. (2009). Measures of emotion: A review. Cognition and Emotion, 23(2), Article 2. https://doi.org/10.1080/02699930802204677

McCall, C., Hildebrandt, L. K., Bornemann, B., & Singer, T. (2015). Physiophenomenology in retrospect: Memory reliably reflects physiological arousal during a prior threatening experience. Consciousness and Cognition, 38, 60–70. https://doi.org/10.1016/j.concog.2015.09.011

McCorry, L. K. (2007). Physiology of the Autonomic Nervous System. American Journal of Pharmaceutical Education, 71(4). https://www.ncbi.nlm.nih.gov/pmc/articles/PMC1959222/

Menon, V. (2015). Salience Network. In Brain Mapping: An Encyclopedic Reference (Vol. 2, pp. 597–611). https://doi.org/10.1016/B978-0-12-397025-1.00052-X

Menon, V., & Uddin, L. Q. (2010). Saliency, switching, attention and control: A network model of insula function. Brain Structure & Function, 214(5–6), 655–667.

https://doi.org/10.1007/s00429-010-0262-0

Meuleman, B., & Rudrauf, D. (2021). Induction and Profiling of Strong Multi-Componential Emotions in Virtual Reality. IEEE Transactions on Affective Computing, 12(1), 189–202. https://doi.org/10.1109/TAFFC.2018.2864730

Mikutta, C., Altorfer, A., Strik, W., & Koenig, T. (2012). Emotions, Arousal, and Frontal Alpha Rhythm Asymmetry During Beethoven's 5th Symphony. Brain Topography, 25(4), 423–430. https://doi.org/10.1007/s10548-012-0227-0

Moosmann, M., Ritter, P., Krastel, I., Brink, A., Thees, S., Blankenburg, F., Taskin, B., Obrig, H., & Villringer, A. (2003). Correlates of alpha rhythm in functional magnetic resonance imaging and near infrared spectroscopy. NeuroImage, 20(1), 145–158. https://doi.org/10.1016/S1053-8119(03)00344-6

Motyka, P., Grund, M., Forschack, N., Al, E., Villringer, A., & Gaebler, M. (2019). Interactions between cardiac activity and conscious somatosensory perception. Psychophysiology, 56(10), e13424. https://doi.org/10.1111/psyp.13424

Nummenmaa, L., Hyönä, J., & Calvo, M. G. (2006). Eye movement assessment of selective attentional capture by emotional pictures. Emotion, 6(2), 257–268. https://doi.org/10.1037/1528-3542.6.2.257

Nummenmaa, L., Hyönä, J., & Calvo, M. G. (2009). Emotional scene content drives the saccade generation system reflexively. Journal of Experimental Psychology: Human Perception and Performance, 35(2), 305–323. https://doi.org/10.1037/a0013626

Ohl, S., Wohltat, C., Kliegl, R., Pollatos, O., & Engbert, R. (2016). Microsaccades Are Coupled to Heartbeat. Journal of Neuroscience, 36(4), 1237–1241. https://doi.org/10.1523/JNEUROSCI.2211-15.2016

Okon-Singer, H., Lichtenstein-Vidne, L., & Cohen, N. (2013). Dynamic modulation of emotional processing. Biological Psychology, 92(3), 480–491. https://doi.org/10.1016/j.biopsycho.2012.05.010

Olbrich, S., Mulert, C., Karch, S., Trenner, M., Leicht, G., Pogarell, O., & Hegerl, U. (2009). EEG-vigilance and BOLD effect during simultaneous EEG/fMRI measurement. NeuroImage, 45(2), 319–332. https://doi.org/10.1016/j.neuroimage.2008.11.014

Palomba, D., Sarlo, M., Angrilli, A., Mini, A., & Stegagno, L. (2000). Cardiac responses associated with affective processing of unpleasant film stimuli. International Journal of Psychophysiology, 36(1), 45–57. https://doi.org/10.1016/S0167-8760(99)00099-9

Park, H.-D., & Blanke, O. (2019). Heartbeat-evoked cortical responses: Underlying mechanisms, functional roles, and methodological considerations. NeuroImage, 197, 502–511.

https://doi.org/10.1016/j.neuroimage.2019.04.081

Pascual-Marqui, R. D. (2007). Discrete, 3D distributed, linear imaging methods of electric neuronal activity. Part 1: Exact, zero error localization (arXiv:0710.3341). arXiv. https://doi.org/10.48550/arXiv.0710.3341

Paton, J. F. R., Boscan, P., Pickering, A. E., & Nalivaiko, E. (2005). The yin and yang of cardiac autonomic control: Vago-sympathetic interactions revisited. Brain Research Reviews, 49(3), 555–565. https://doi.org/10.1016/j.brainresrev.2005.02.005

Perakakis, P. (2019). HEPLAB: a Matlab graphical interface for the preprocessing of the heartbeat-evoked potential.

Petzschner, F. H., Weber, L. A., Wellstein, K. V., Paolini, G., Do, C. T., & Stephan, K. E. (2019). Focus of attention modulates the heartbeat evoked potential. NeuroImage, 186, 595–606. https://doi.org/10.1016/j.neuroimage.2018.11.037

Pollatos, O., Herbert, B. M., Mai, S., & Kammer, T. (2016). Changes in interoceptive processes following brain stimulation. Philosophical Transactions of the Royal Society B: Biological Sciences, 371(1708), 20160016. https://doi.org/10.1098/rstb.2016.0016

Raimondo, F., Rohaut, B., Demertzi, A., Valente, M., Engemann, D. A., Salti, M., Fernandez Slezak, D., Naccache, L., & Sitt, J. D. (2017). Brain–heart interactions reveal consciousness in noncommunicating patients. Annals of Neurology, 82(4), 578–591. https://doi.org/10.1002/ana.25045

Reyes del Paso, G. A., Langewitz, W., Mulder, L. J. M., van Roon, A., & Duschek, S. (2013). The utility of low frequency heart rate variability as an index of sympathetic cardiac tone: A review with emphasis on a reanalysis of previous studies. Psychophysiology, 50(5), 477–487. https://doi.org/10.1111/psyp.12027

Riva, G., Mantovani, F., Capideville, C. S., Preziosa, A., Morganti, F., Villani, D., Gaggioli, A., Botella, C., & Alcañiz, M. (2007). Affective interactions using virtual reality: The link between presence and emotions. Cyberpsychology and Behavior, 10(1), 45–56. https://doi.org/10.1089/cpb.2006.9993

Rottenberg, J., & Gross, J. J. (2003). When emotion goes wrong: Realizing the promise of affective science. Clinical Psychology: Science and Practice, 10(2), 227–232. https://doi.org/10.1093/clipsy.bpg012

Russell, J. A. (2003). Core affect and the psychological construction of emotion. Psychological Review, 110(1), 145–172. https://doi.org/10.1037/0033-295x.110.1.145

Samide, R., Cooper, R. A., & Ritchey, M. (2020). A database of news videos for investigating the dynamics of emotion and memory. Behavior Research Methods, 52(4), 1469–1479.

https://doi.org/10.3758/s13428-019-01327-w

Sammler, D., Grigutsch, M., Fritz, T., & Koelsch, S. (2007). Music and emotion: Electrophysiological correlates of the processing of pleasant and unpleasant music. Psychophysiology, 44(2), 293–304. https://doi.org/10.1111/j.1469-8986.2007.00497.x

Sander, D., Grandjean, D., & Scherer, K. R. (2005). A systems approach to appraisal mechanisms in emotion. Neural Networks, 18(4), 317–352. https://doi.org/10.1016/j.neunet.2005.03.001

Schandry, R., Sparrer, B., & Weitkunat, R. (1986). From the heart to the brain: A study of heartbeat contingent scalp potentials. International Journal of Neuroscience, 30(4), 261–275. https://doi.org/10.3109/00207458608985677

Scherg, M., Berg, P., Nakasato, N., & Beniczky, S. (2019). Taking the EEG Back Into the Brain: The Power of Multiple Discrete Sources. Frontiers in Neurology, 10. https://www.frontiersin.org/articles/10.3389/fneur.2019.00855

Schubring, D., Kraus, M., Stolz, C., Weiler, N., Keim, D. A., & Schupp, H. (2020). Virtual Reality Potentiates Emotion and Task Effects of Alpha/Beta Brain Oscillations. Brain Sciences, 10(8), Article 8. https://doi.org/10.3390/brainsci10080537

Seeley, W. W. (2019). The Salience Network: A Neural System for Perceiving and Responding to Homeostatic Demands. The Journal of Neuroscience : The Official Journal of the Society for Neuroscience, 39(50), Article 50. https://doi.org/10.1523/JNEUROSCI.1138-17.2019

Seth, A. K. (2013). Interoceptive inference, emotion, and the embodied self. Trends in Cognitive Sciences, 17(11), 565–573. https://doi.org/10.1016/j.tics.2013.09.007

Shaffer, F., McCraty, R., & Zerr, C. L. (2014). A healthy heart is not a metronome: An integrative review of the heart's anatomy and heart rate variability. Frontiers in Psychology, 5. https://www.frontiersin.org/articles/10.3389/fpsyg.2014.01040

Siegel, E. H., Sands, M. K., Van den Noortgate, W., Condon, P., Chang, Y., Dy, J., Quigley, K. S., & Barrett, L. F. (2018). Emotion fingerprints or emotion populations? A meta-analytic investigation of autonomic features of emotion categories. Psychological Bulletin, 144(4), 343. https://doi.org/10.1037/bul0000128

Signoret-Genest, J., Schukraft, N., L. Reis, S., Segebarth, D., Deisseroth, K., & Tovote, P. (2023). Integrated cardio-behavioral responses to threat define defensive states. Nature Neuroscience, 26(3), Article 3. https://doi.org/10.1038/s41593-022-01252-w

Sutherland, M. R., & Mather, M. (2018). Arousal (but not valence) amplifies the impact of salience. Cognition and Emotion, 32(3), 616–622. https://doi.org/10.1080/02699931.2017.1330189

Task Force. (1996). Heart rate variability: Standards of measurement, physiological interpretation and clinical use. Task Force of the European Society of Cardiology and the North American Society of Pacing and Electrophysiology. Circulation, 93(5), 1043–1065.

Thayer, J. F., & Lane, R. D. (2000). A model of neurovisceral integration in emotion regulation and dysregulation. Journal of Affective Disorders, 61(3), 201–216. https://doi.org/10.1016/S0165-0327(00)00338-4

Thayer, J. F., & Lane, R. D. (2009). Claude Bernard and the heart–brain connection: Further elaboration of a model of neurovisceral integration. Neuroscience & Biobehavioral Reviews, 33(2), 81–88. https://doi.org/10.1016/j.neubiorev.2008.08.004

Todd, R. M., Taylor, M. J., Robertson, A., Cassel, D. B., Doesberg, S. M., Lee, D. H., Shek, P. N., & Pang, E. W. (2014). Temporal-Spatial Neural Activation Patterns Linked to Perceptual Encoding of Emotional Salience. PLOS ONE, 9(4), e93753. https://doi.org/10.1371/journal.pone.0093753

Treisman, A. M. (1969). Strategies and models of selective attention. Psychological Review, 76, 282–299. https://doi.org/10.1037/h0027242

Valenza, G., Allegrini, P., Lanatà, A., & Scilingo, E. P. (2012). Dominant Lyapunov exponent and approximate entropy in heart rate variability during emotional visual elicitation. Frontiers in Neuroengineering, 5. https://doi.org/10.3389/fneng.2012.00003

Valenza, G., Citi, L., Saul, J. P., & Barbieri, R. (2018). Measures of sympathetic and parasympathetic autonomic outflow from heartbeat dynamics. Journal of Applied Physiology, 125(1), 19–39. https://doi.org/10.1152/japplphysiol.00842.2017

Van Diepen, R. M., Foxe, J. J., & Mazaheri, A. (2019). The functional role of alpha-band activity in attentional processing: The current zeitgeist and future outlook. Current Opinion in Psychology, 29, 229–238. https://doi.org/10.1016/j.copsyc.2019.03.015

Villena-González, M., Moënne-Loccoz, C., Lagos, R. A., Alliende, L. M., Billeke, P., Aboitiz, F., López, V., & Cosmelli, D. (2017). Attending to the heart is associated with posterior alpha band increase and a reduction in sensitivity to concurrent visual stimuli. Psychophysiology, 54(10), 1483–1497. https://doi.org/10.1111/psyp.12894

Vuilleumier, P. (2005). How brains beware: Neural mechanisms of emotional attention. Trends in Cognitive Sciences, 9(12), 585–594. https://doi.org/10.1016/j.tics.2005.10.011

Warner, H. R., & Cox, A. (1962). A mathematical model of heart rate control by sympathetic and vagus efferent information. Journal of Applied Physiology. https://doi.org/10.1152/jappl.1962.17.2.349

Winkler, I., Debener, S., Müller, K.-R., & Tangermann, M. (2015). On the influence of high-pass

filtering on ICA-based artifact reduction in EEG-ERP. Annual International Conference of the IEEE Engineering in Medicine and Biology Society. IEEE Engineering in Medicine and Biology Society. Annual International Conference, 2015, 4101–4105. https://doi.org/10.1109/EMBC.2015.7319296

Wundt, W. (1897). Outline of psychology (pp. xviii, 342). Wilhelm Engelmann. https://doi.org/10.1037/12908-000

Zaccaro, A., Perrucci, M. G., Parrotta, E., Costantini, M., & Ferri, F. (2022). Brain-heart interactions are modulated across the respiratory cycle via interoceptive attention. NeuroImage, 262, 119548. https://doi.org/10.1016/j.neuroimage.2022.119548